Inactive Methyl Indole-3-Acetic Acid Ester Can Be Hydrolyzed and Activated by Several Esterases Belonging to the *At*MES Esterase Family of Arabidopsis[1][W][OA]

Yue Yang[2], Richard Xu, Choong-je Ma[3], A. Corina Vlot[4], Daniel F. Klessig, and Eran Pichersky*

Department of Molecular, Cellular and Developmental Biology, University of Michigan, Ann Arbor, Michigan 48109–1048 (Y.Y., R.X., C.M., E.P.); and Boyce Thompson Institute for Plant Research, Ithaca, New York 14853 (A.C.V., D.F.K.)

The plant hormone auxin (indole-3-acetic acid [IAA]) is found both free and conjugated to a variety of carbohydrates, amino acids, and peptides. We have recently shown that IAA could be converted to its methyl ester (MeIAA) by the Arabidopsis (*Arabidopsis thaliana*) enzyme IAA carboxyl methyltransferase 1. However, the presence and function of MeIAA in vivo remains unclear. Recently, it has been shown that the tobacco (*Nicotiana tabacum*) protein SABP2 (salicylic acid binding protein 2) hydrolyzes methyl salicylate to salicylic acid. There are 20 homologs of SABP2 in the genome of Arabidopsis, which we have named *At*MES (for methyl esterases). We tested 15 of the proteins encoded by these genes in biochemical assays with various substrates and identified several candidate MeIAA esterases that could hydrolyze MeIAA. MeIAA, like IAA, exerts inhibitory activity on the growth of wild-type roots when applied exogenously. However, the roots of Arabidopsis plants carrying T-DNA insertions in the putative MeIAA esterase gene *AtMES17* (*At3g10870*) displayed significantly decreased sensitivity to MeIAA compared with wild-type roots while remaining as sensitive to free IAA as wild-type roots. Incubating seedlings in the presence of [^{14}C]MeIAA for 30 min revealed that *mes17* mutants hydrolyzed only 40% of the [^{14}C]MeIAA taken up by plants, whereas wild-type plants hydrolyzed 100% of absorbed [^{14}C]MeIAA. Roots of Arabidopsis plants overexpressing *At*MES17 showed increased sensitivity to MeIAA but not to IAA. Additionally, *mes17* plants have longer hypocotyls and display increased expression of the auxin-responsive DR5:β-glucuronidase reporter gene, suggesting a perturbation in IAA homeostasis and/or transport. *mes17-1/axr1-3* double mutant plants have the same phenotype as *axr1-3*, suggesting MES17 acts upstream of AXR1. The protein encoded by *AtMES17* had a K_m value of 13 μM and a K_{cat} value of 0.18 s^{-1} for MeIAA. *AtMES17* was expressed at the highest levels in shoot apex, stem, and root of Arabidopsis. Our results demonstrate that MeIAA is an inactive form of IAA, and the manifestations of MeIAA in vivo activity are due to the action of free IAA that is generated from MeIAA upon hydrolysis by one or more plant esterases.

Indole-3-acetic acid (IAA), also known as auxin, is a plant hormone involved in many aspects of plant growth and development, such as embryogenesis, vascular differentiation, fruit set and development, and senescence (Woodward and Bartel, 2005; Teale et al., 2006; Delker et al., 2008). Plants utilize a variety of mechanisms to spatially and temporally regulate IAA concentrations and gradients, including de novo synthesis, degradation, transport, and synthesis and hydrolysis of various IAA conjugates (Normanly, 1997; Ljung et al., 2002; Woodward and Bartel, 2005).

IAA is known to be conjugated to sugars, amino acids, and peptides, and some enzymes that catalyze these conjugating reactions have been characterized (Jackson et al., 2001; Staswick et al., 2005). Some conjugates such as IAA-Asp and IAA-Glu are not able to induce auxin responses when applied exogenously and therefore are considered inactive auxin and intermediates in IAA degradation (Ljung et al., 2002; Woodward and Bartel, 2005). Recently, a rice (*Oryza sativa*) *GH3-8* gene encoding IAA-amino acid synthetase has been shown to promote basal immunity in rice by converting active IAA to inactive IAA-Asp and thus reducing the auxin-induced cell wall loosening (Ding et al., 2008). Other IAA conjugates such as IAA-Leu and IAA-Ala induce auxin responses when applied exogenously to plants. However, the hydrolytic cleavage of these compounds parallels the activity (Bartel and Fink, 1995; Ljung et al., 2002). These findings have led to suggestions that these conjugates per se are biologically inactive, and any response obtained in the assay reflected the degree of hydrolysis and the activity of the released free hormone.

[1] This work was supported by the National Science Foundation (Arabidopsis 2010 project grant no. MCB–0312466 to E.P., and grant no. IOB–0525360 to D.F.K.).

[2] Present address: Department of Plant Biology, Michigan State University, East Lansing, MI 48824.

[3] Present address: School of Bioscience and Biotechnology, Kangwon National University, Chuncheon 200–701, Korea.

[4] Present address: Max Planck Institute for Plant Breeding Research, 50829 Cologne, Germany.

* Corresponding author; e-mail lelx@umich.edu.

The author responsible for distribution of materials integral to the findings presented in this article in accordance with the policy described in the Instructions for Authors (www.plantphysiol.org) is: Eran Pichersky (lelx@umich.edu).

[W] The online version of this article contains Web-only data.

[OA] Open Access articles can be viewed online without a subscription.

www.plantphysiol.org/cgi/doi/10.1104/pp.108.118224

A family of hydrolases that acts on IAA-amino acid conjugates and releases IAA from some IAA-amino acid conjugates has been identified in Arabidopsis (*Arabidopsis thaliana*; LeClere et al., 2002; Rampey et al., 2004). The hydrolyzable IAA conjugates have been proposed to function as storage form to allow the plants to quickly release active IAA when necessary. While the transport of any IAA conjugates has rarely been reported, IAA-inositol has been shown to be transported from the endosperm to shoot in *Zea mays* at a rate much faster than that of free IAA and there hydrolyzed to yield free IAA (Nowacki and Bandurski, 1980).

We have recently discovered an IAA carboxy methyltransferase (IAMT1) in Arabidopsis and several other species that can methylate IAA to form the ester methyl indole-3-acetate (MeIAA; Zubieta et al., 2003; Qin et al., 2005; Zhao et al., 2008). Furthermore, disruption of the expression levels of *IAMT1* led to phenotypes indicative of disruption of IAA homeostasis (Qin et al., 2005). MeIAA has rarely been reported as an endogenous IAA metabolite in plants (Narasimhan et al., 2003), probably due to its low abundance or fast turnover, and therefore its in vivo function remains unknown. MeIAA had been used as a substitute for IAA in physiological studies (Zimmerman and Hitchcock, 1937), and it has been observed that various auxin signaling mutants show decreased sensitivity to exogenously applied MeIAA as well as to IAA (Qin et al., 2005), suggesting that MeIAA and IAA share similar signaling components. Therefore, either MeIAA itself could initiate the auxin signaling pathway, or it must be hydrolyzed to IAA to exert hormonal function. If MeIAA hydrolysis occurs in planta, the reaction is likely to be catalyzed by one or more carboxylesterases.

Carboxylesterases catalyze the hydrolysis of a C-O ester linkage in a wide range of compounds, and structural analyses have shown that such enzymes are all members of the α/β hydrolase "superfamily" (Nardini and Dijkstra, 1999). Carboxylesterases have been extensively studied in animals and microbes. However, the physiological role and substrate specificity of few plant carboxylesterases have been identified. Several putative plant proteins, including those encoded by tobacco (*Nicotiana tabacum*) *hsr203J*, the tomato (*Solanum lycopersicum*) and pea (*Pisum sativum*) homologs of *hsr203J*, and *PrMC3* from *Pinus radiata* and *pepEST* from pepper (*Capsicum annuum*; Pontier et al., 1994, 1998; Walden et al., 1999; Ichinose et al., 2001; Ko et al., 2005) have been annotated as carboxylesterases based on homology with fungal esterases but with little direct biochemical evidence (Baudouin et al., 1997). Marshall et al. (2003), in turn, searched the Arabidopsis genome, which has several hundred members of the α/β hydrolase superfamily, for genes encoding proteins with the highest similarities to these previously annotated plant carboxylesterases. This bioinformatic search identified a branch of the α/β hydrolase superfamily containing 20 genes, which were collectively named the *At*CXE family (Marshall et al., 2003). However, the in vivo substrates of none of the enzymes in the *At*CXE family have been experimentally determined. Recently, two proteins belonging to the α/β hydrolase superfamily have been identified in *Gentiana triflora* and implicated in cold response, but their in vivo substrates remain unknown (Hikage et al., 2007).

Recently, we have demonstrated that a tobacco protein required for development of systemic acquired resistance, SABP2 (originally identified as salicylic acid binding protein 2), is a methyl salicylate (MeSA) esterase (Kumar and Klessig, 2003; Forouhar et al., 2005). The amino acid sequence of SABP2 shares 46% to 56% similarity to two other confirmed methyl esterases from plants, methyl jasmonate (MeJA) esterase (MJE) from tomato and polyneuridine aldehyde esterase (PNAE) from the medicinal plant *Rauvolfia serpentina* (Dogru et al., 2000; Stuhlfelder et al., 2004; Forouhar et al., 2005). Bioinformatic analysis of the Arabidopsis genome revealed 20 genes encoding proteins with relatively high sequence similarities to SABP2 (Forouhar et al., 2005; Yang et al., 2006a). These proteins are distinct from the group of 20 *At*CXE proteins, and their sequence similarity to known methylesterases suggests that they too may be methylesterases and may perhaps be involved in the hydrolysis of MeSA, MeJA, or MeIAA in Arabidopsis (Yang et al., 2006a).

Here, we show that some of the proteins in this group of putative Arabidopsis methylesterases, which we have named MES (for methyl esterases), are able to hydrolyze MeIAA. Analysis of mutants with T-DNA insertions in the *At*MES genes indicates that at least one *At*MES (*At*MES17) is capable of hydrolyzing MeIAA in vivo. We used this mutant to demonstrate that MeIAA itself is an inactive form of IAA.

RESULTS

The Arabidopsis Genome Has 20 *MES* Genes

A search of the Arabidopsis genome for genes encoding proteins with the highest identity to tobacco SABP2 (MeSA esterase), tomato MJE, and *R. serpentina* PNAE identified 20 genes forming a close clade within the α/β hydrolase superfamily, which we named *AtMES1* to *AtMES20* (Fig. 1; Table I). The amino acid sequences of the *At*MES proteins, which range in length from 256 to 444 amino acids (with the exception of the proteins encoded by *AtMES19* and *20*, which are likely to be pseudogenes; see below), share 30% to 57% similarity with tobacco SABP2, 31% to 42% similarity with tomato MJE, and 29% to 49% similarity with *R. serpentina* PNAE. The tree topology of the *At*MES family shows the presence of three clusters of genes, which we have named subfamilies 1, 2, and 3 (Fig. 1). Members of the previously annotated plant carboxylesterases (CXE) family, including tobacco *hsr203J*, *PrMC3*, and three *AtCXE* genes (*AtCXE1*, *-2*, and *-19*), are more

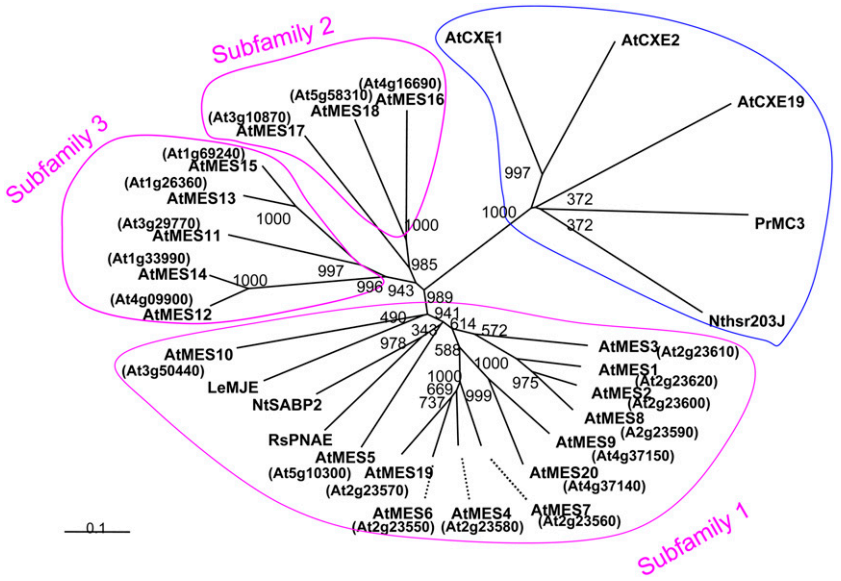

Figure 1. An unrooted neighbor-joining tree showing the phylogenetic relationships among *At*MES proteins and other carboxylesterases. The tree was constructed with protein sequences of 20 Arabidopsis MES members (*At*MES1–*At*MES20), NtSABP2, *R. serpentina* PNAE, and LeMJE. Protein sequences of CXE family members *AtCXE1*, *-2*, and *-19*, *Nthsr203J*, and *P. radiata* (*Pr*) *MC3* were also included in the phylogenetic analysis. Bootstrap values were calculated from 1,000 replicates. The three clusters of sequences that contain all the *At*MES sequences were designated as subfamilies 1, 2, and 3. Analysis using maximum parsimony (not shown) gave a tree with the same four major branches.

divergent, and they cluster into a clade that is distant from the *AtMES* family (Fig. 1).

The sequence alignment of *At*MES1 to *At*MES20 revealed that the catalytic triad Ser-His-Asp, a characteristic feature of the α/β hydrolase fold family, is conserved in 15 of these proteins (Fig. 2). In the protein sequences of *At*MES11, *At*MES13, and *At*MES15, the conserved Ser in the catalytic triad is replaced by Asp, a substitution previously found in active α/β hydrolases in animals (Holmquist, 2000). *At*MES19 and *At*MES20 lack part of the N-terminal or C-terminal region, respectively, and are therefore likely to be inactive enzymes.

Substrate Specificities of 15 MES Esterases

To examine whether the *AtMES* genes encode functional esterases, we obtained full-length cDNAs of 15 *AtMES* genes, expressed the cDNAs in *Escherichia coli*, and tested the recombinant proteins for esterase activity. Because *AtMES19* and *AtMES20* were likely to be pseudogenes, they were not tested. Three other

Table I. *Substrate specificities of AtMES proteins*

*At*MES family members (*At*MES1–*At*MES20) are listed with the respective gene identification numbers. Fifteen heterologously expressed *At*MES proteins were assayed for esterase activities with PNPA, MeIAA, MeSA, MeJA, $MeGA_4$, and $MeGA_9$, as described in "Materials and Methods." +, Active; −, not active; n.d., not determined.

Name	Gene ID	PNPA	MeIAA	MeSA	MeJA	$MeGA_4$	$MeGA_9$
*At*MES1	At2g23620	+	+	+	+	−	−
*At*MES2	At2g23600	+	+	+	+	−	−
*At*MES3	At2g23610	+	+	−	+	−	−
*At*MES4	At2g23580	+	−	+	−	−	−
*At*MES5	At5g10300	−	−	−	−	−	−
*At*MES6	At2g23550	n.d.	n.d.	n.d.	n.d.	n.d.	n.d.
*At*MES7	At2g23560	+	+	+	−	−	−
*At*MES8	At2g23590	+	−	−	−	−	−
*At*MES9	At4g37150	+	+	+	+	−	−
*At*MES10	At3g50440	−	−	−	+	−	−
*At*MES11	At3g29770	−	−	−	−	−	−
*At*MES12	At4g09900	−	−	−	−	−	−
*At*MES13	At1g26360	n.d.	n.d.	n.d.	n.d.	n.d.	n.d.
*At*MES14	At1g33990	−	−	−	−	−	−
*At*MES15	At1g69240	n.d.	n.d.	n.d.	n.d.	n.d.	n.d.
*At*MES16	At4g16690	+	+	−	+	−	−
*At*MES17	At3g10870	+	+	−	−	−	−
*At*MES18	At5g58310	−	+	−	−	−	−
*At*MES19	At2g23570	n.d.	n.d.	n.d.	n.d.	n.d.	n.d.
*At*MES20	At4g37140	n.d.	n.d.	n.d.	n.d.	n.d.	n.d.

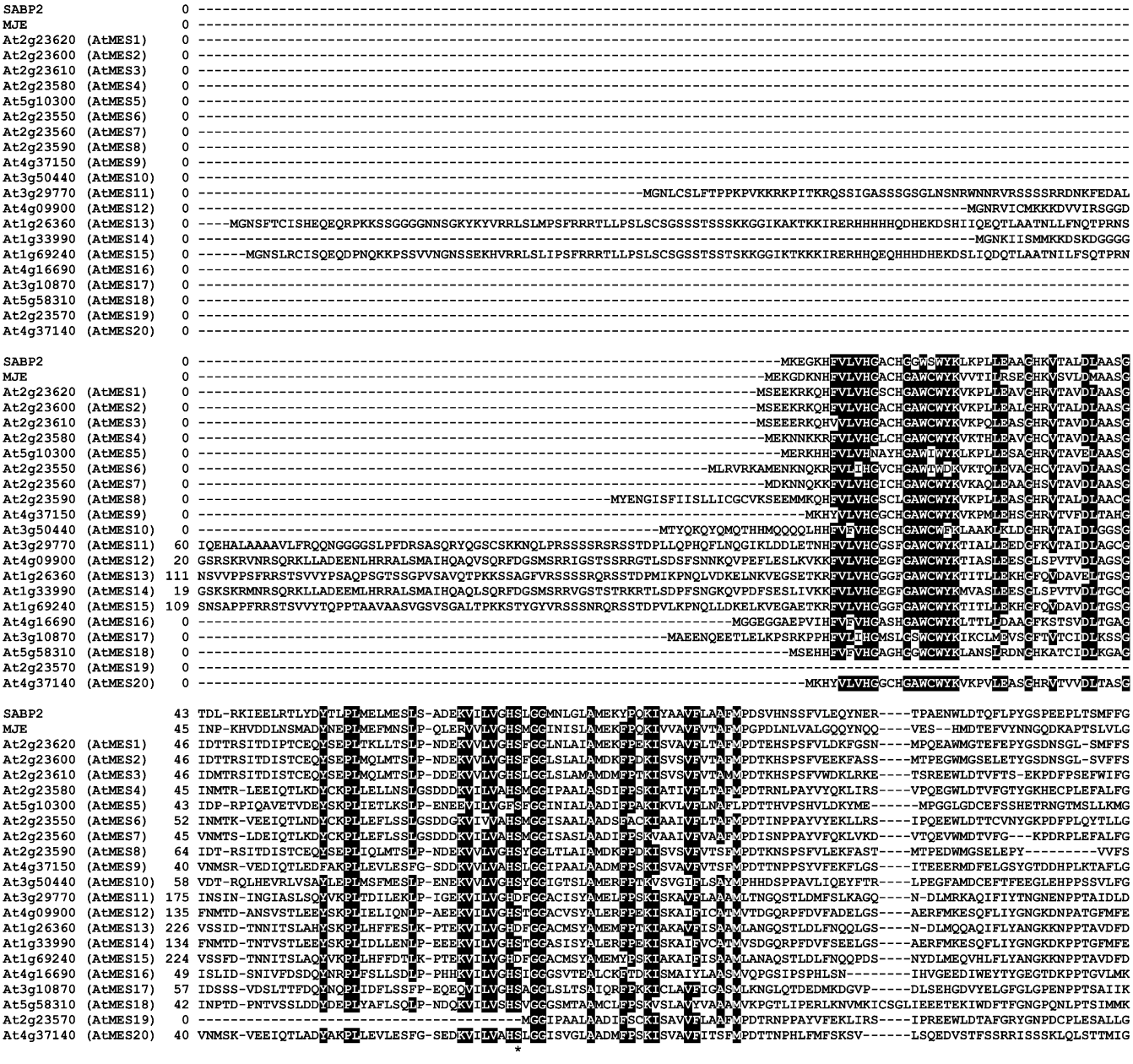

Figure 2. (*Legend appears on following page.*)

*At*MES proteins, *At*MES6, *At*MES13, and *At*MES15, were also not tested, because we were not able to obtain full-length cDNAs.

When the 15 *At*MES esterases were tested with the chymotryptic synthetic substrate *p*-nitrophenyl acetate (PNPA), *At*MES1, *At*MES2, *At*MES3, *At*MES4, *At*MES7, *At*MES8, *At*MES9, *At*MES16, and *At*MES17 showed activity (Table I). Because the *At*MES proteins are homologs of SABP2 and MJE, esterases that hydrolyze the methylated plant hormones MeSA and MeJA, respectively, we further examined whether the *At*MES proteins are active with known methylated plant hormones, including MeIAA, MeSA, MeJA, $MeGA_4$, and $MeGA_9$ (Shulaev et al., 1997; Chen et al., 2003; Qin et al., 2005; Yang et al., 2006a; Varbanova et al., 2007). To assess whether the *At*MES proteins are active with any of these substrates, we carried out preliminary assays for each protein with a number of substrates present at a concentration of 1 mM. Reactions that resulted in product formation that was at least 3 times the value found in control assays (using boiled enzyme) were scored "+" as indicating enzymatic activity (Table I).

Among the 15 esterases tested, *At*MES1, *At*MES2, *At*MES3, *At*MES7, *At*MES9, *At*MES16, *At*MES17, and *At*MES18 displayed hydrolase activity with MeIAA, while *At*MES4, *At*MES5, *At*MES8, *At*MES10, *At*MES11, *At*MES12, and *At*MES14 could not hydrolyze MeIAA (Table I). In addition, *At*MES1, *At*MES2, *At*MES4, *At*MES7, and *At*MES9 displayed MeSA hydrolase activity, while *At*MES1, *At*MES2, *At*MES3, *At*MES9, *At*MES10, and *At*MES16 were active with MeJA. None of the 15 *At*MES esterases was active with $MeGA_4$ or $MeGA_9$. *At*MES5, *At*MES8, *At*MES11, *At*MES12, and *At*MES14 were not active with any of these methylated hormones.

AtMES17 Null Mutant Plants Are More Resistant Than Wild Type to the Root Inhibition Activity of Exogenously Supplied MeIAA and They Are Defective in Hydrolysis of Such MeIAA in Vivo

Because *At*MES1, *At*MES2, *At*MES3, *At*MES7, *At*MES9, *At*MES16, *At*MES17, and *At*MES18 could all hydrolyze MeIAA in vitro, we examined whether they possess MeIAA hydrolase activity in vivo. It has been previously shown that both IAA and MeIAA inhibit root growth in wild-type Arabidopsis seedlings when applied exogenously (Zimmerman and Hitchcock, 1937; Qin et al., 2005), but it has not been determined if MeIAA itself is active or whether the apparent activity of MeIAA is due to its hydrolysis in planta, giving rise to active IAA.

T-DNA insertional mutants of *AtMES1*, *AtMES9*, *AtMES16*, and *AtMES17* were obtained as described in "Materials and Methods," including two independent mutant lines each for both *AtMES*16 and *AtMES*17. There was no T-DNA insertional mutant of *AtMES3* reported, and the several T-DNA insertions reported for *AtMES2*, *AtMES7*, and *AtMES18* turned out upon further examination (described in "Materials and Methods") not to abolish gene transcriptions (data not shown).

All mutant lines as well as wild-type Arabidopsis plants were next grown on one-half-strength Murashige and Skoog (MS) medium containing various concentrations of MeIAA or no MeIAA, and their root lengths were measured after 7 d. While in unsupplemented medium, root length of an *At*MES17 T-DNA mutant *mes17-1* (SALK_092550) seedlings were similar to that of wild type; in the presence of MeIAA concentrations ranging from 0.01 to 1 μM, root length of mutant seedlings was consistently longer than the root length of wild-type seedlings (Fig. 3B). For example, at 0.5 μM MeIAA, a concentration that inhibits the root growth of wild-type Arabidopsis by 85% on average, wild-type seedlings had an average root length of 4.1 mm and *mes17-1* plants had an average root length of 12 mm, 3 times as long as that of the wild type (Fig. 3, A and B). Similar results were obtained with a second independent *AtMES17* T-DNA mutant, *mes17-2* (SAIL-503-c03; data not shown). The root lengths of *AtMES1*, *AtMES9*, and *AtMES16* mutant lines grown on MeIAA were the same as wild type. All mutant plants, including the *mes17-1* and *mes17-2*, when grown on one-half-strength MS medium containing different concentrations of IAA, showed no statistically significant difference in root length from that of wild-type plants, although the *mes17* mutants appeared to have a slightly diminished response to IAA (Fig. 3, C and D).

To examine directly the fate of exogenously added MeIAA in wild-type and *Atmes*17 mutant plants, we soaked plants in a 0.5 μM solution of [^{14}C]MeIAA and examined the total amount of [^{14}C]label taken up by the plant and the relative amounts of [^{14}C]MeIAA remaining in the plant tissues. After 30 min of incubation, wild-type plants had no [^{14}C]MeIAA left, but *Atmes17-1* plants still contained 58.5% $\pm$ 16.5% of the [^{14}C]label taken up in the form of MeIAA (Fig. 4).

We also obtained several lines that overexpress *AtMES17* under the control of the 35S promoter and tested them for sensitivity to MeIAA and IAA treatments. When *At*MES17-overexpressing plants of three independent lines were grown in the presence of 0.5 μM MeIAA for 7 d, their root growth was more severely inhibited than that of wild-type seedlings (see Fig. 5A for one of the lines). However, both types of seedlings had a similar root length in the presence of 0.5 μM IAA (Fig. 5B), suggesting that the increased root inhibition of MeIAA on *MES17*-overexpressing plants was caused by increased auxin concentration derived from increased rate of MeIAA hydrolysis.

Figure 2. Multiple sequence alignment of tobacco SABP2, tomato MJE, and the 20 Arabidopsis *At*MES. The sequence alignment was constructed using ClustalX program (Thompson et al., 1997). Identical amino acids at a given position in 17 or more proteins are shown in white letters on black. The catalytic triad residues are indicated by asterisks.

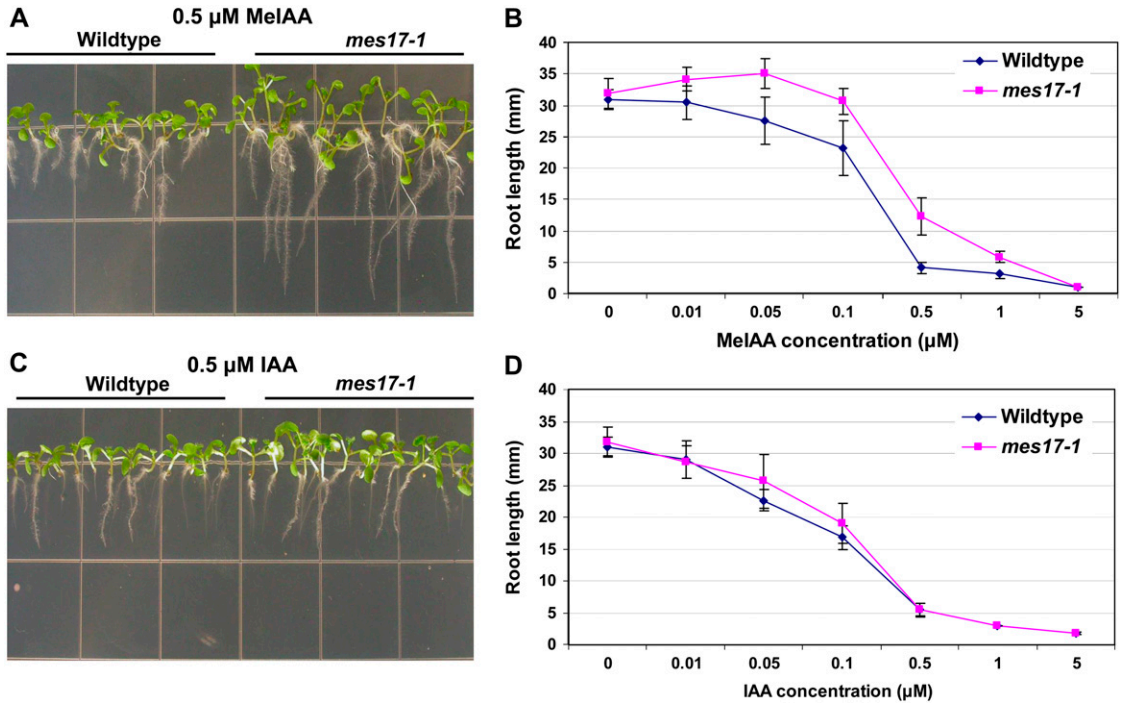

Figure 3. Plants with a null mutation in *AtMES17* are more resistant to MeIAA but not to IAA. A, Seedlings were grown on one-half-strength MS medium containing 0.5 μM MeIAA for 7 d. B, Root length (mean ± SD, $n \geq 20$) of wild-type and *mes17-1* plants grown for 7 d on one-half-strength MS medium containing various concentrations of MeIAA. C, Seedlings were grown on one-half-strength MS medium containing 0.5 μM IAA for 7 d. D, Root length (mean ± SD, $n \geq 20$) of wild-type and *mes17-1* plants grown for 7 d on one-half-strength MS medium containing various concentrations of IAA.

Atmes17 Null Mutants Have a Longer Hypocotyl

We observed that *mes17-1* mutant plants grown in soil had, in general, longer hypocotyls than wild-type plants. The hypocotyls of 4-week-old *mes17-1* plants were on average 32% longer than that of the wild type (Fig. 6). Statistical analysis performed by Student's *t* test returned *P* values $<1 \times 10^{-9}$, indicating that the differences are significant. When grown on one-half-strength MS medium under continuous light for 8 d, *mes17-1* and *mes17-2* mutants had hypocotyls longer on average by 29% than that of wild-type seedlings (Fig. 6), with statistical analysis indicating that the differences are significant (*P* values $<1 \times 10^{-5}$). When grown on one-half-strength MS medium in the dark, however, the hypocotyl lengths of *mes17-1* and *mes17-2* mutants were the same as that of wild type (Fig. 6). With the exception of hypocotyl length, *mes17* mutants grown under normal conditions did not display any obvious phenotypic differences compared to wild type.

The DR5:GUS Reporter Gene Is More Highly Expressed in *Atmes17* Null Mutants Compared with Wild-Type Plants

DR5 is a synthetic auxin response element, and the DR5:GUS reporter has been widely used as a marker to study the endogenous distribution of auxin (Ulmasov et al., 1997; Ottenschlager et al., 2003). We constructed *mes17* null mutant plants carrying the DR5:GUS reporter gene and tested them for GUS activity. *mes17* null plants had much stronger GUS staining overall than wild-type plants, including in the shoot apex and in the root primordia and leaf tip (Fig. 7).

mes17-1/*axr1-3* Double Mutant Plants Have the Same Phenotype as *axr1-3*

Plants homozygous for the allele *axr1-3*, which carries a missense mutation in the AXR1 gene, display resistance to exogenous auxin, as well as a variety of morphological defects due to compromised auxin signaling (Lincoln et al., 1990; Leyser et al., 1993). We have

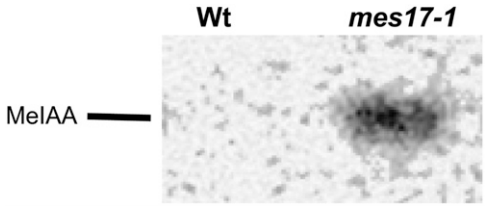

Figure 4. Plants with a null mutation in *AtMES17* hydrolyze exogenously supplied MeIAA at a much lower efficiency than wild-type plants. Wild-type and *mes17-1* seedlings were incubated in a 0.5 μM solution of [^{14}C]MeIAA for 30 min. [^{14}C]MeIAA absorbed by the plants was extracted and analyzed by radio-TLC. The position of an authentic MeIAA standard is also shown.

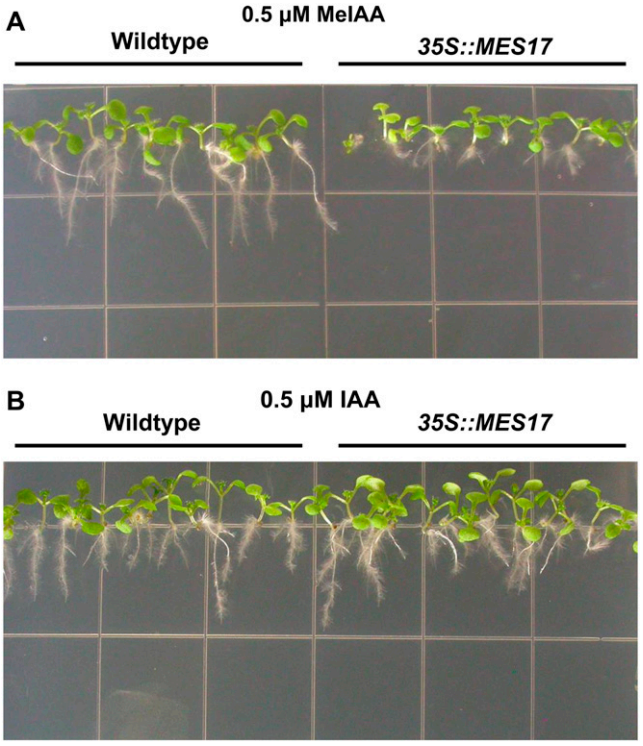

Figure 5. Plants overexpressing *AtMES17* are more sensitive to MeIAA treatment but not to IAA. Wild-type plants and plants overexpressing *AtMES17* were grown on one-half-strength MS medium containing 0.5 μM MeIAA (A) or IAA (B) for 7 d.

previously shown that *axr1-3* mutants also have reduced sensitivity to MeIAA (Qin et al., 2005), suggesting that MeIAA shares similar signaling components as IAA. We therefore constructed plants that were homozygous for both *mes17-1* and *axr1-3* and tested them for their phenotype and response to IAA and MeIAA. While *mes17-1* mutant had a longer hypocotyl than wild type when grown in one-half-strength MS medium in light, *axr1-3* has a shorter hypocotyl than wild type (Fig. 8; Jensen et al., 1998). The hypocotyl length of *mes17-1/axr1-3* was shorter than that of wild type, similar with the hypocotyl length of *axr1-3* mutant (Fig. 8). In addition, *mes17-1/axr1-3* mutant plants had the same morphological phenotype as the *axr1-3* mutant line, which includes irregular rosette leaves, reduced height, and reduced fertility (data not shown). When plants were tested for their responses to the root growth inhibition activity of IAA and MeIAA, the *mes17-1/axr1-3* double mutant displayed reduced sensitivity to both IAA and MeIAA, as did *axr1-3* (data not shown).

Biochemical Characterization of *At*MES17

Because *At*MES17 displays MeIAA hydrolase activity in vitro and likely does so in vivo, we performed a more detailed in vitro kinetic analysis of the *E. coli*-expressed and purified *At*MES17. *At*MES17 displayed hydrolase activity toward MeIAA but not MeJA, MeSA, or MeGAs (Table I). *At*MES17 displayed the highest MeIAA hydrolase activity at pH 8.5 and about 60% of the highest activity at pH 6.5 or 9.5. However, at pH 8.0 or higher, nonenzymatic hydrolysis of MeIAA was also observed. We therefore used buffers with pH 7.5, which gave 93% of the maximal enzymatic activity and no observable nonenzymatic hydrolysis. Under these conditions, *At*MES17 had a K_m value of 13 μM and a K_{cat} value of 0.18 s^{-1} for MeIAA. The hydrolase activity was strongly inhibited (44%–75%) by 5 mM Fe^{2+}, Fe^{3+}, Zn^{2+}, and Cu^{2+}, and mildly inhibited by 5 mM Ca^{2+} and Mn^{2+} (20% and 34%, respectively). At 5 mM concentration, Na^+, Mg^{2+}, K^+, and NH_4^+ had no effects on the hydrolase activity.

Expression Pattern of *AtMES17*

Real-time reverse transcription (RT)-PCR analysis showed that the expression of *AtMES17* in 10-d-old seedlings is approximately 5-fold higher in the region of the shoot apex than in the rest of the hypocotyl (Fig. 9). When *AtMES17* transcript levels in the 8-week mature plants were examined, the highest expression levels were observed in stems, followed by roots, flowers, rosette leaves, and siliques, and no *AtMES17* transcripts were detectable in cauline leaves (Fig. 9).

DISCUSSION

The Arabidopsis MES Methylesterase Family

We have identified a family of 20 Arabidopsis proteins that we have designated the *At*MES family, based

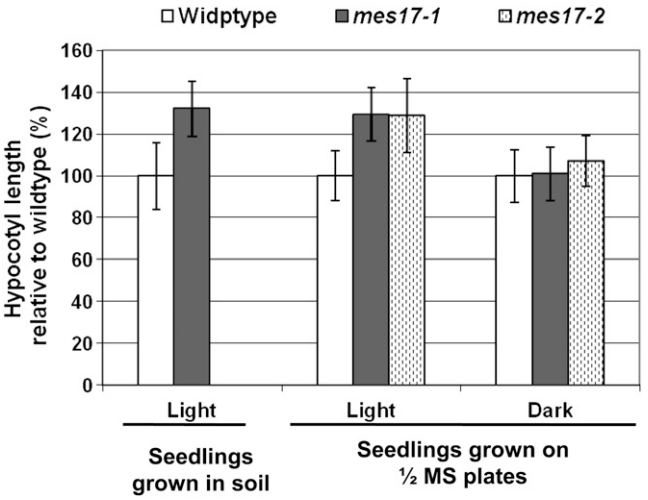

Figure 6. Plants carrying a null mutation in *AtMES17* have longer hypocotyls. Left, Analysis of hypocotyl lengths of 4-week-old wild-type and *mes17-1* Arabidopsis plants grown in soil. Right, Analysis of the hypocotyl length of wild-type, *mes17-1*, and *mes17-2* seedlings grown on one-half-strength MS medium under continuous light for 8 d or in the dark for 4 d. Hypocotyl lengths of the seedlings grown on one-half-strength MS plates were measured with Image J as described in "Materials and Methods." The mean value and SD were calculated from 20 samples.

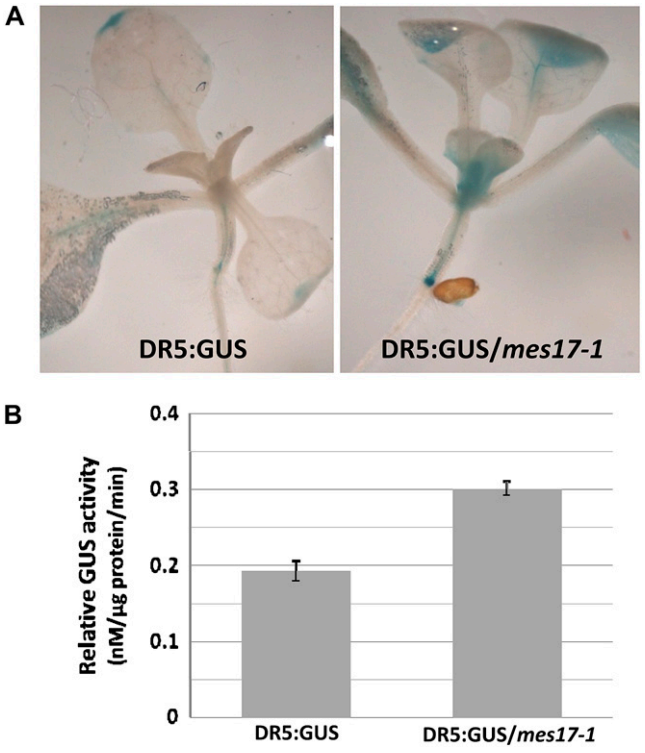

Figure 7. Histochemical staining of GUS activity in DR5:GUS and DR5:GUS/*mes17-1* seedlings. A, DR5:GUS seedlings and DR5:GUS/*mes17-1* seedlings were stained for GUS activity for 16 h. B, Quantitative GUS assay of DR5:GUS and DR5:GUS/*mes17-1* seedlings. The mean value and SD of GUS activity were calculated from three replicates and represented as nanomoles of 4-methyl umbelliferone per milligram protein per minute, as described in "Materials and Methods."

on the sequence similarity of these proteins to experimentally identified methyl esterases, including the tobacco MeSA esterase SABP2 (*Nt*SABP2) and the tomato MJE (*Le*MJE). This *At*MES family is distinct from the previously annotated *At*CXE family (Fig. 1), yet both families belong to the α/β hydrolase superfamily, which is characterized by the structurally conserved "canonical" α/β hydrolase fold and catalytic residues (Nardini and Dijkstra, 1999).

Most members of the *At*MES family encode proteins of approximately 250 amino acids, similarly to *Nt*SABP2 and *Le*MJE. *At*MES11, *At*MES12, *At*MES13, *At*MES14, and *At*MES15 contain an extra region of 90 to 190 amino acids at their N termini (Fig. 2). This N-terminal extension does not appear to constitute a targeting signal peptide, suggesting that these *At*MES proteins are localized in the cytosol like the rest of the members in the family. The *At*MES11, *At*MES12, *At*MES13, *At*MES14, and *At*MES15 proteins also cluster into a close clade within the *At*MES family (subfamily 3, Fig. 1), and so far we have not been able to ascribe any enzymatic activity to any of the proteins in this subfamily.

Because the *At*MES proteins are closely related to *Le*MJE and *Nt*SABP2, we hypothesized that members of the *At*MES family could encode MeIAA esterase(s). Of the members of the *At*MES family that we tested, eight *At*MES proteins were found to be active with MeIAA, and they all belong to subfamilies 1 and 2. Some of these proteins also hydrolyze other methyl esters under the experimental conditions used in this study, and it is likely that many, and perhaps all, of the *At*MES proteins would be found to use multiple substrates upon a more extensive survey of substrates.

AtMES17 Encodes an Esterase Capable of Hydrolyzing MeIAA, Which Is Not Itself Active

We further showed that *AtMES17* encodes an esterase that efficiently and specifically hydrolyzes MeIAA to IAA in vitro and is likely to do so in vivo as well. The kinetic parameters of *At*MES17 are comparable to previously characterized esterases (Forouhar et al., 2005), indicating that MeIAA is likely to be a relevant substrate for *At*MES17 in planta. As pointed out above, although MES17 showed activity with only MeIAA in our limited survey, we cannot yet conclude that MeIAA is its only substrate.

The growth of roots of two independent *mes17* mutants was much less inhibited by MeIAA than was wild-type root growth (Fig. 3A). However, both *mes17* null mutants responded similarly as did wild type to the root inhibition activity of IAA (Fig. 3B), indicating normal auxin signaling in these mutants. Incubating seedlings in the presence of [^{14}C]MeIAA also revealed that *mes17* mutants were much less efficient in hydrolyzing [^{14}C]MeIAA than wild-type plants (Fig. 4). We thus conclude that the response of Arabidopsis seedlings to the root inhibition activity of MeIAA is at least partly due to the hydrolytic activity of *At*MES17. The observations that some hydrolysis of [^{14}C]MeIAA occurred in the *mes17* mutant line and that the root growth of *mes17* mutants retained some response to the inhibitory activity of MeIAA also indicate that there are other esterases in addition to

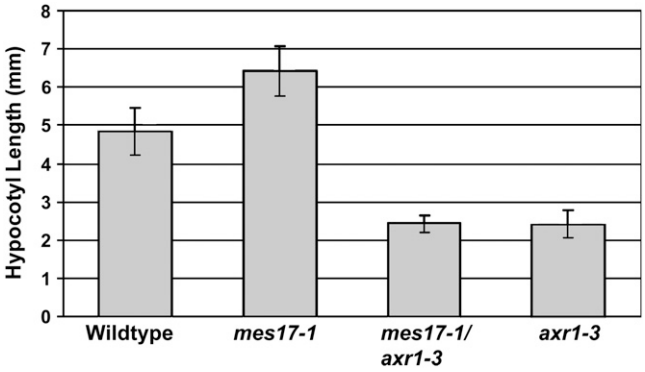

Figure 8. The *mes17/axr1-3* double mutant has the same hypocotyl length as *axr1-3*. Plants were grown on one-half-strength MS medium under continuous light for 9 d. The hypocotyl lengths of the seedlings were measured with Image J as described in "Materials and Methods." The mean value and SD were calculated from 20 samples.

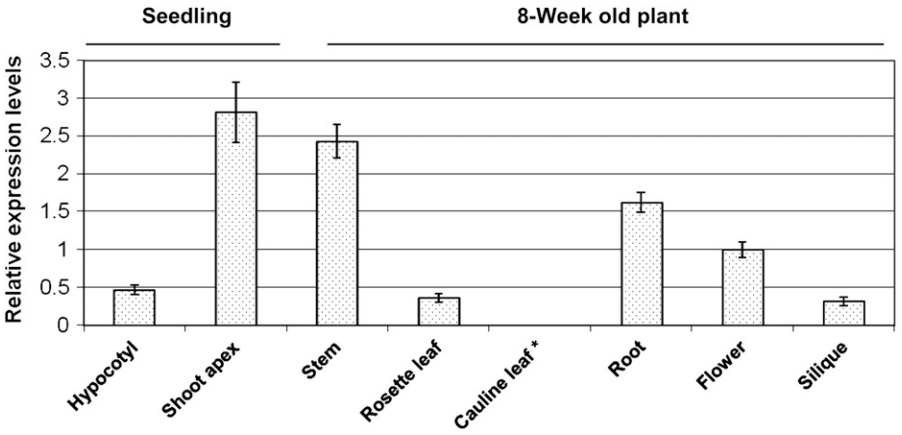

Figure 9. Real-time RT-PCR analysis of *AtMES17* transcript levels in different plant organs at different developmental stages. *AtMES17* transcript levels were normalized to the levels of ubiquitin gene expression in respective samples. The levels of *AtMES17* transcript in flowers were arbitrarily set to 1.0. Data are plotted as means ± SD. *, Below the detection limit.

*At*MES17 that participate in MeIAA hydrolysis in Arabidopsis, consistent with our finding that other *At*MES proteins could hydrolyze MeIAA in vitro. These proteins include *At*MES16 and *At*MES18, which have the highest sequence similarities to *At*MES17. However, we obtained two independent T-DNA insertional lines of *AtMES16* and observed that both of these null mutants responded to MeIAA similarly to wild type, including in the root growth assay. Microarray data indicates that transcript levels of *AtMES17* in roots are more than 10 times higher than those of *AtMES16* (AtGenExpress Visualization Tool; Schmid et al., 2005). In addition, the double mutant *mes16/mes17-1* was phenotypically indistinguishable from the *mes17-1* mutant in all organs or developmental stages (data not shown). We were unable to obtain a T-DNA insertion in *At*MES18. It remains to be determined whether *At*MES16 or other *At*MES can hydrolyze MeIAA in vivo.

The much-reduced (although not completely abolished) response of roots of *mes17* mutants in the root inhibition assay with exogenously supplied MeIAA coupled with the observation that these mutants are much less efficient in the hydrolysis of MeIAA also suggest that the inhibition is due to IAA and not MeIAA. Consistent with this interpretation, when *AtMES17* was overexpressed, its roots were even more sensitive to MeIAA than wild-type plants (Fig. 5), likely because MeIAA was hydrolyzed in these plants even faster than in wild type. The observation that the *mes17-1/axr1-3* double mutant plants have the same phenotype as *axr1-3* is also consistent with the putative role of MES17 in producing IAA, which acts upstream of AXR1. A similar albeit more extensive analysis of the effects of MeIAA treatment on *axr1* and other auxin response mutants has also concluded that MeIAA is likely to be inactive by itself (Li et al., 2008). In addition, the recently solved structure of the auxin receptor TIR1 supports the notion that MeIAA is not an active auxin, because it was shown that the carboxyl group of the IAA molecule interacts with two residues in the binding pocket of TIR1, docking IAA to the bottom of the pocket (Tan et al., 2007). MeIAA has a methyl ester group instead of a carboxyl group and therefore is not likely to be accommodated in the binding site of TIR1 to initiate TIR1-mediated auxin signaling. Analogous to our finding, it was recently shown that silencing of a tobacco MJE (*Na*MJE) reduced MeJA- but not JA-induced herbivore resistance, indicating that the resistance elicited by MeJA treatment is directly elicited not by MeJA but by its demethylated product, JA (Wu et al., 2008).

Possible Role of MeIAA in Arabidopsis

mes17-1 mutants have longer hypocotyls than wild-type plants. The regulation of hypocotyl length is a complex process that is under the influence of many factors, including light, nutrients, and hormones such as IAA, ethylene, and brassinosteroids (Jensen et al., 1998; Collett et al., 2000; Vandenbussche et al., 2005). Earlier physiological studies have shown that auxin promotes the growth of excised hypocotyl segments from various plant species (Evans, 1985). Several Arabidopsis mutants that accumulate increased overall auxin levels also have longer hypocotyls than wild type, although the auxin gradient may be more important than its actual concentration (Boerjan et al., 1995; Zhao et al., 2001, 2002). In addition, Jensen et al. (1998) have demonstrated that auxin transport from the shoot apex to the root is required for hypocotyl elongation in Arabidopsis during development in the light.

In seedlings, *AtMES17* is expressed at highest levels in the shoot apex, but it is also expressed at lower levels elsewhere (Fig. 9). *mes17-1* plants display a stronger auxin response in the shoot apex as well as in other parts of the plant (as assessed by the DR5:GUS reporter system; Fig. 7). Although it seems paradoxical that *mes17* mutants appear to have higher levels of IAA, it may be that the higher GUS staining in this line indicates a higher rate of transport of IAA rather than a higher level of IAA concentration, brought about by higher but transient and localized concentrations of MeIAA due to the decrease in (but not complete absence of) overall MeIAA esterase activity. Methylation of IAA to enhance its transport (and subsequent

hydrolysis by MES enzymes) would be analogous to the transport of SA as biologically inactive MeSA from the site of infection to distal tissue for development of systemic acquired resistance (Park et al., 2007). For this explanation to be valid, however, it would appear necessary to postulate that there are distinct types of cells, probably in close proximity to each other, that contain either IAA methylation activity or MeIAA esterase activity.

A high-resolution spatial map depicting auxin concentration as well as activities of MES17 and IAMT is needed to validate this hypothesis. Recently, a cell type-specific microarray analysis has shown that in a given area of roots, genes involved in auxin biosynthesis are expressed in different cells than genes regulating auxin homeostasis or auxin transport (Brady et al., 2007). Transient methylation of IAA and small local differences in expression of *MES17* (and *IAMT*) among populations of cells may also explain our failure to detect differences in MeIAA concentration between wild-type, *mes17*, and 35S::IAMT lines, which all contain MeIAA levels that are barely detectable (Y. Yang, unpublished data). The expression of *YUCCA* genes, involved in biosynthesis of auxin, are localized to small populations of cells, and the actual differences in IAA concentrations in *yucca* mutants are also difficult to demonstrate, despite strong defects in organ formation in these mutants (Cheng et al., 2007). Alternatively, it is possible that other auxin biosynthetic pathways are induced in response to the loss of MES17 activity in the shoot apex as well as in other parts of the plants.

In conclusion, our results suggest that MES17 functions in auxin homeostasis in vivo and that MeIAA itself is not an active auxin. Because MeIAA is more nonpolar than IAA, MeIAA could more easily diffuse across membranes, and it is therefore possible that transport of IAA (in the form of MeIAA) to neighboring cells or even to more distant targets could be enhanced, where it could be hydrolyzed back to the active auxin IAA by esterases belonging to the MES family.

MATERIALS AND METHODS

Plant Material and Growth Conditions

Wild-type Arabidopsis (*Arabidopsis thaliana*) ecotype Columbia was used in all experiments. The *AtMES17* full-length cDNA was ligated into pCHF3 vector (Varbanova et al., 2007) using the Gateway system (Hartley et al., 2000). The resulting 35S::*AtMES17* construct was then introduced into wild-type Arabidopsis using *Agrobacterium*-mediated transformation by the floral dip method (Clough and Bent, 1998). Three independent homozygous transgenic lines were selected by examining the pattern of kanamycin resistance in T2 and T3 generations, and overexpression of *AtMES17* in these homozygous lines was confirmed by northern blot (D'Auria et al., 2002).

Arabidopsis plants grown in soil were under 16-h-light/8-h-dark cycles at 22°C. Arabidopsis plants grown on one-half-strength MS medium (Murashige and Skoog, 1962) were subjected to constant light at 22°C.

Chemicals

All chemicals were purchased from Sigma. MeIAA and IAA were dissolved in 95% ethanol to make stock solutions of different concentrations. Stock solutions were then diluted 1:1,000 into one-half-strength MS medium, and the medium was poured into square plates. Plates containing chemicals were wrapped in aluminum foil and stored at 4°C before use.

Protein Expression and Purification

Isolation of *At*MES cDNAs and construction of *Escherichia coli* expression vectors of all *AtMES* genes, except *At*MES11, *At*MES12, and *At*MES18, are described elsewhere (A.C. Vlot and D.F. Klessig, unpublished data). Full-length cDNA of *At*MES11 (U22904), *At*MES12 (U15905), and *At*MES18 (U50042) were obtained from the Arabidopsis Biological Resource Center (ABRC), and subcloned into pENTR/D-TOPO (Invitrogen) and subsequently p-His-9 vector (a Gateway adapted derivative of pET28a). The plasmid containing the respective *At*MES cDNA was transformed into *E. coli* and expressed as previously described (Nam et al., 1999), with the following minor modifications. All expression constructs in this study were transformed into the *E. coli* cell line BL21 Codon plus. *E. coli* cells were grown to an OD_{600} of 0.4, then induced with 0.4 mm isopropylthio-β-galactoside and grown at 18°C overnight. The cell lysate used in esterase enzyme assays or protein purification was first examined by SDS-PAGE to ensure that the protein encoded by the cDNA was expressed.

For protein purification, nickel-nitrilotriacetic acid agarose (Qiagen) was loaded into a column and washed with 10 bed volumes of water followed by 10 bed volumes of lysis buffer (50 mM Tris-HCl, pH 8.0, 500 mM NaCl, 20 mM imidazole, pH 8.0, 20 mM β-mercaptoethanol, 10% [v/v] glycerol, and 1% [v/v] Tween 20). Ten bed volumes of cell lysate was passed over the column and subsequently washed with 10 bed volumes of lysis buffer, and 20 bed volumes of wash buffer (50 mM Tris-HCl, pH 8.0, 500 mM NaCl, 20 mM imidazole, pH 8.0, 20 mM β-mercaptoethanol, and 10% [v/v] glycerol). The protein was eluted with elution buffer (50 mM Tris-HCl, pH 8.0, 500 mM NaCl, 250 mM imidazole, pH 8.0, 20 mM β-mercaptoethanol, and 10% [v/v] glycerol) and collected in 0.5-mL fractions. After being examined by SDS-PAGE, elution fractions containing the most abundant purified proteins were pooled and concentrated by centrifugation in the Amicon Ultra-4 centrifugal filter (Millipore). Concentrated proteins were finally resuspended in a buffer containing 50 mM Tris-HCl, pH 8.0, 10 mM NaCl, 20 mM β-mercaptoethanol, and 10% (v/v) glycerol. All purification procedures were performed at 4°C.

Esterase Enzyme Assay

The chymotryptic substrate PNPA was dissolved in acetonitrile to make a stock solution of 100 mM. An assay was prepared containing 50 mM Tris-HCl, pH 7.5, 0.05% Triton X-100, 1 mM PNPA, and 200 μL expression lysate. Control assays were set up in parallel with denatured protein. Esterase activity was estimated by the rate of hydrolysis determined spectrophometrically at 410 nM. The assay was carried out at room temperature, and OD_{410} values were measured at 2-min intervals up to 30 min. All assays were performed in duplicate. An *At*MES protein was considered active when the reaction product determined by OD_{410} was at least 3 times that of the control assay.

Esterase assays with MeIAA, MeSA, MeJA, MeGA4, and MeGA9 as substrates were performed using the coupled methyltransferase assay, as previously described (Forouhar et al., 2005). All assays were performed in triplicate.

For kinetic analysis of *At*MES17, the amount of IAA generated from the esterase assay was quantified by HPLC analysis on a Waters 2690 Separations Module. HPLC separation of MeIAA and IAA was achieved over a Waters Nova-Pak C18 column, using an 8-min linear gradient from 65% acetonitrile in 1.5% phosphoric acid to 90% acetonitrile, with the flow rate set at 1 mL/min and the column temperature set to 30°C. In-line UV light spectra (200–450 nm) were obtained using an attached Waters 996 photodiode array detector. Eluting compounds were identified by comparison of both UV light spectra and elution volume with authentic MeIAA and IAA. IAA peak area detected at 278.4 nM (the maximum absorption wavelength for IAA) was plotted onto a standard curve created at identical parameters to calculate the product of each reaction.

[^{14}C]MeIAA Uptake and in Vivo Hydrolysis Assays

[^{14}C]MeIAA was produced by incubating IAA with [^{14}C]SAM and IAMT under assay conditions described previously (Zubieta et al., 2003). Seedlings (8 d old) were incubated in a 100-μL solution containing 0.5 μM [^{14}C]MeIAA and 50 mM Tris-HCl, pH 7.5. After 30 min of incubation, the solution was removed, the seedlings were washed with 1 mL of distilled, deionized water

three times, and then ground with a pestle in 100 μL of Tris-HCl buffer. [^{14}C]MeIAA in the plants was then extracted with ethyl acetate and analyzed by radio-TLC and in a scintillation counter as previously described (Fridman et al., 2005). [^{14}C]MeIAA was loaded on the same TLC plate to show the position of MeIAA. Each experiment was repeated three times and results calculated on per fresh weight basis.

Characterization of *At*MES17 Kinetic Parameters

Appropriate enzyme concentrations and incubation time were chosen so that the reaction velocity was linear over time with no more than 10% of the substrate consumed during the time period. The determination of kinetic parameters was as described (Yang et al., 2006b), except that 50 mM BisTris propane, pH 7.5, was used to examine all steady-state kinetics, because control assays prepared with denatured enzyme indicated that nonenzymatic hydrolysis occurs at pH 8.0 and increases as pH increases.

Screening of T-DNA Insertional Mutants

The following T-DNA insertional mutants were obtained from ABRC: Salk_006044 (*At*MES1), Salk_030442 (*At*MES9), Salk_151578 (*At*MES16), Salk_139756 (*At*MES16), Salk_092550 (*At*MES17), and SAIL-503-c03 (*At*MES17). The T-DNA insertion sites in these *AtMES* genes were verified first by PCR using T-DNA-specific primer SALKLBb1 (5′-GCGTGGACCGCTTGCTGCAACT-3′, for SALK lines) or SAILLB3 (5′-TAGCATCTGAATTTCATAACCAATCT-3′, for SAIL lines) and the genomic primers designed for each T-DNA insertional line as follows: Salk_006044 forward (5′-CACCGAACACTCACCATCCTTCG-3′) and reverse (5′-TTAAACGAATTTGTCCGCGATTTTCAG-3′); Salk_030442 forward (5′-ATGAAGCATTATGTGCTAGTTCACGGAGGC-3′) and reverse (5′-TTAGGGATATTTATCAGCAATCTTTAGAAG-3′); Salk_151578 forward (5′-TTACTAACTCACCTCTCTTCTTCTTCG-3′) and reverse (5′-ATACGCTAAGGCATCGAAGGG-3′); Salk_139756 forward (5′CTCTCTTGTCCGATCTCCCTCC-3′) and reverse (5′-CCCTGGATTGCTTCGCATG-3′); Salk_092550 forward (5′-GCGTTTGACAAATGTGACAAGGC-3′) and reverse (5′-GGTTTGATAATAGCACTGGTGGG-3′); and SAIL-503-c03 forward (5′-ATGGCGGAGGAGAATC-3′) and reverse (5′-TTAGATAGAACCGACGGAAACGGC-3′). PCR results were verified by sequencing. All homozygous T-DNA insertional lines were confirmed by PCR with specific primers and subsequent Southern blot. RT-PCR was done with RNA extracted from homozygous lines to ensure absence of the respective gene transcript (see Supplemental Fig. S1 for *mes17* mutants). Homozygous T-DNA insertional lines were also obtained for *AtMES2* (Salk_050266), *AtMES7* (Salk_054303, Salk_036791), and *AtMES18* (CS826062). However, full-length gene transcripts were detectable in these mutants.

Measurement of Root Length and Hypocotyl Length

The root length of seedlings was measured with a ruler, and at least 20 measurements were taken to calculate the mean and SD values. Hypocotyl lengths of 4-week-old plants grown in soil were measured with a ruler. To measure hypocotyl length of seedlings grown on plates, seedlings were gently lifted with forceps from plates onto acetate sheets and digitized with a flat-bed scanner at a resolution of 1,200 dpi. Seedling scans were analyzed by ImageJ 1.37v software (National Institutes of Health), through which the hypocotyl lengths of seedling were measured. Twenty seedlings were analyzed for each measurement to calculate mean and SD values.

Real-Time RT-PCR Analysis

RNA extraction, purification, and real-time RT-PCR were performed as described (Varbanova et al., 2007). Shoot apex and hypocotyl were collected from 10-d-old plants grown in soil. Flowers, siliques, stems, rosette leaves, cauline leaves, and roots were collected from 8-week-old flowering plants grown in soil. *AtMES17* gene-specific primers were designed as follows: forward 5′-GTTTTGGTCTAGGACCGGAGAATC-3′ and reverse 5′-CCAAGGAACATTCCTGTTGAGG-3′.

DR5:GUS Reporter Analysis

DR5:GUS/*mes17* plants were obtained by crossing the DR5:GUS line into the *mes17-1* mutant line. Plants homozygous for both DR5:GUS and *mes17-1* were analyzed for GUS activity and compared to that of wild-type DR5:GUS. Seedlings were grown on one-half-strength MS medium for 8 d and incubated in GUS staining solution (100 mM sodium phosphate buffer, pH 6.8, 10 mM EDTA, 0.2% Triton X-100, and 0.2 mg/mL 5-bromo-4-chloro-3-indolyl-β-D-glucuronide) for 16 h, after which chlorophyll were extracted with 75% ethanol for 24 h. Quantitative GUS assay was carried out as described by Nakamura et al. (2003) except that 1.3 mM 4-methylumbelliferyl-β-D-glucuronide was used and the assay was carried out for 32 min.

Supplemental Data

The following materials are available in the online version of this article.

Supplemental Figure S1. *mes17-1* and *mes17-2* are null mutants of *AtMES17*.

ACKNOWLEDGMENTS

We thank Dr. Mark Estelle at the University of Indiana for providing the *axr1-3* line. We thank Dr. Yunde Zhao at the University of California at San Diego for providing the DR5:GUS line.

Received February 22, 2008; accepted April 23, 2008; published May 8, 2008.

LITERATURE CITED

Bartel B, Fink G (1995) ILR1, an amidohydrolase that releases active indole-3-acetic acid from conjugates. Science **268:** 1745–1748

Baudouin E, Charpenteau M, Roby D, Marco Y, Ranjeva R, Ranty B (1997) Functional expression of a tobacco gene related to the serine hydrolase family-esterase activity towards short-chain dinitrophenyl acylesters. Eur J Biochem **248:** 700–706

Boerjan W, Cervera MT, Delarue M, Beeckman T, Dewitte W, Bellini C, Caboche M, Onckelen HV, Montagu MV, Inze D (1995) superroot, A recessive mutation in *Arabidopsis*, confers auxin overproduction. Plant Cell **7:** 1405–1419

Brady SM, Orlando DA, Lee JY, Wang JY, Koch J, Dinneny JR, Mace D, Ohler U, Benfey PN (2007) A high-resolution root spatiotemporal map reveals dominant expression patterns. Science **318:** 801–806

Chen F, D'Auria JC, Tholl D, Ross JR, Gershenzon J, Noel JP, Pichersky E (2003) An *Arabidopsis thaliana* gene for methylsalicylate biosynthesis, identified by a biochemical genomics approach, has a role in defense. Plant J **36:** 577–588

Cheng Y, Dai X, Zhao Y (2007) Auxin synthesized by the YUCCA flavin monooxygenases is essential for embryogenesis and leaf formation in *Arabidopsis*. Plant Cell **19:** 2430–2439

Clough SJ, Bent AF (1998) Floral dip: a simplified method for Agrobacterium-mediated transformation of *Arabidopsis thaliana*. Plant J **16:** 735–743

Collett CE, Harberd NP, Leyser O (2000) Hormonal interactions in the control of Arabidopsis hypocotyl elongation. Plant Physiol **124:** 553–562

D'Auria JC, Chen F, Pichersky E (2002) Characterization of an acyltransferase capable of synthesizing benzylbenzoate and other volatile esters in flowers and damaged leaves of *Clarkia breweri*. Plant Physiol **130:** 466–476

Delker C, Raschke A, Quint M (2008) Auxin dynamics: the dazzling complexity of a small molecule's message. Planta **227:** 929–941

Ding X, Cao Y, Huang L, Zhao J, Xu C, Li X, Wang S (2008) Activation of the indole-3-acetic acid amido synthetase GH3-8 suppresses expansin expression and promotes salicylate- and jasmonate-independent basal immunity in rice. Plant Cell **20:** 228–240

Dogru E, Warzecha H, Seibel F, Haebel S, Lottspeich F, Stöckigt J (2000) The gene encoding polyneuridine aldehyde esterase of monoterpenoid indole alkaloid biosynthesis in plants is an ortholog of the alpha/beta hydrolase super family. Eur J Biochem **267:** 1397–1406

Evans ML (1985) The action of auxin on plant-cell elongation. Crc Crit Rev Plant Sci **2:** 317–365

Forouhar F, Yang Y, Kumar D, Chen Y, Fridman E, Park SW, Chiang Y, Acton TB, Montelione GT, Pichersky E, et al (2005) Structural and biochemical studies identify tobacco SABP2 as a methyl salicylate esterase and implicate it in plant innate immunity. Proc Natl Acad Sci USA **102:** 1773–1778

Fridman E, Wang J, Iijima Y, Froehlich JE, Gang DR, Ohlrogge J, Pichersky E (2005) Metabolic, genomic, and biochemical analyses of glandular trichomes from the wild tomato species *Lycopersicon hirsutum*

identify a key enzyme in the biosynthesis of methylketones. Plant Cell **17:** 1252–1267

Hartley JL, Temple GF, Brasch MA (2000) DNA cloning using in vitro site-specific recombination. Genome Res **10:** 1788–1795

Hikage T, Saitoh Y, Tanaka-Saito C, Hagami H, Satou F, Shimotai Y, Nakano Y, Takahashi M, Takahata Y, Tsutsumi K (2007) Structure and allele-specific expression variation of novel alpha/beta hydrolase fold proteins in gentian plants. Mol Genet Genomics **278:** 95–104

Holmquist M (2000) Alpha beta-hydrolase fold enzymes structures, functions and mechanisms. Curr Protein Pept Sci **1:** 209–235

Ichinose Y, Hisayasu Y, Sanematsu S, Ishiga Y, Seki H, Toyoda K, Shiraishi T, Yamada T (2001) Molecular cloning and functional analysis of pea cDNA E86 encoding homologous protein to hypersensitivity-related hsr203J. Plant Sci **160:** 997–1006

Jackson RG, Lim EK, Li Y, Kowalczyk M, Sandberg G, Hoggett J, Ashford DA, Bowles DJ (2001) Identification and biochemical characterization of an Arabidopsis indole-3-acetic acid glucosyltransferase. J Biol Chem **276:** 4350–4356

Jensen PJ, Hangarter RP, Estelle M (1998) Auxin transport is required for hypocotyl elongation in light-grown but not dark-grown Arabidopsis. Plant Physiol **116:** 455–462

Ko MK, Jeon WB, Kim KS, Lee HH, Seo HH, Kim YS, Oh BJ (2005) A Colletotrichum gloeosporioides-induced esterase gene of nonclimacteric pepper (*Capsicum annuum*) fruit during ripening plays a role in resistance against fungal infection. Plant Mol Biol **58:** 529–541

Kumar D, Klessig DF (2003) High-affinity salicylic acid-binding protein 2 is required for plant innate immunity and has salicylic acid-stimulated lipase activity. Proc Natl Acad Sci USA **100:** 16101–16106

LeClere S, Tellez R, Rampey RA, Matsuda SPT, Bartel B (2002) Characterization of a family of IAA-amino acid conjugate hydrolases from Arabidopsis. J Biol Chem **277:** 20446–20452

Leyser HM, Lincoln CA, Timpte C, Lammer D, Turner J, Estelle M (1993) Arabidopsis auxin-resistance gene AXR1 encodes a protein related to ubiquitin-activating enzyme E1. Nature **364:** 161–164

Li L, Hou X, Tsuge T, Ding M, Aoyama T, Oka A, Gu H, Zhao Y, Qu LJ (2008) The possible action mechanisms of indole-3-acetic acid methyl ester in Arabidopsis. Plant Cell Rep **27:** 575–584

Lincoln C, Britton JH, Estelle M (1990) Growth and development of the Axr1 mutants of *Arabidopsis*. Plant Cell **2:** 1071–1080

Ljung K, Hull AK, Kowalczyk M, Marchant A, Celenza J, Cohen JD, Sandberg G (2002) Biosynthesis, conjugation, catabolism and homeostasis of indole-3-acetic acid in *Arabidopsis thaliana*. Plant Mol Biol **50:** 309–332

Marshall SG, Putterill J, Plummer K, Newcomb R (2003) The carboxylesterase gene family from *Arabidopsis thaliana*. J Mol Evol **V57:** 487–500

Murashige T, Skoog F (1962) A revised medium for rapid growth and bioassays with tobacco tissue cultures. Physiol Plant **15:** 473–497

Nakamura A, Higuchi K, Goda H, Fujiwara MT, Sawa S, Koshiba T, Shimada Y, Yoshida S (2003) Brassinolide induces IAA5, IAA19, and DR5, a synthetic auxin response element in Arabidopsis, implying a cross talk point of brassinosteroid and auxin signaling. Plant Physiol **133:** 1843–1853

Nam KH, Dudareva N, Pichersky E (1999) Characterization of benzylalcohol acetyltransferases in scented and non-scented *Clarkia* species. Plant Cell Physiol **40:** 916–923

Narasimhan K, Basheer C, Bajic VB, Swarup S (2003) Enhancement of plant-microbe interactions using a rhizosphere metabolomics-driven approach and its application in the removal of polychlorinated biphenyls. Plant Physiol **132:** 146–153

Nardini M, Dijkstra BW (1999) Alpha/beta hydrolase fold enzymes: the family keeps growing. Curr Opin Struct Biol **9:** 732–737

Normanly J (1997) Auxin metabolism. Physiol Plant **100:** 431–442

Nowacki J, Bandurski RS (1980) Myoinositol esters of indole-3-acetic-acid as seed auxin precursors of *Zea Mays* L. Plant Physiol **65:** 422–427

Ottenschlager I, Wolff P, Wolverton C, Bhalerao RP, Sandberg G, Ishikawa H, Evans M, Palme K (2003) Gravity-regulated differential auxin transport from columella to lateral root cap cells. Proc Natl Acad Sci USA **100:** 2987–2991

Park SW, Kaimoyo E, Kumar D, Mosher S, Klessig DF (2007) Methyl salicylate is a critical mobile signal for plant systemic acquired resistance. Science **318:** 113–116

Pontier D, Godiard L, Marco Y, Roby D (1994) Hsr203j, A tobacco gene whose activation is rapid, highly localized and specific for incompatible plant/pathogen interactions. Plant J **5:** 507–521

Pontier D, Tronchet M, Rogowsky P, Lam E, Roby D (1998) Activation of hsr203, a plant gene expressed during incompatible plant-pathogen interactions, is correlated with programmed cell death. Mol Plant Microbe Interact **11:** 544–554

Qin G, Gu H, Zhao Y, Ma Z, Shi G, Yang Y, Pichersky E, Chen H, Liu M, Chen Z, et al (2005) Regulation of *Arabidopsis* leaf development by an indole-3-acetic acid carboxyl methyltransferase in *Arabidopsis*. Plant Cell **17:** 2693–2704

Rampey RA, LeClere S, Kowalczyk M, Ljung K, Sandberg G, Bartel B (2004) A family of auxin-conjugate hydrolases that contributes to free indole-3-acetic acid levels during Arabidopsis germination. Plant Physiol **135:** 978–988

Schmid M, Davison TS, Henz SR, Pape UJ, Demar M, Vingron M, Scholkopf B, Weigel D, Lohmann JU (2005) A gene expression map of *Arabidopsis thaliana* development. Nat Genet **37:** 501–506

Shulaev V, Silverman P, Raskin I (1997) Airborne signalling by methyl salicylate in plant pathogen resistance. Nature **385:** 718–721

Staswick PE, Serban B, Rowe M, Tiryaki I, Maldonado MT, Maldonado MC, Suza W (2005) Characterization of an *Arabidopsis* enzyme family that conjugates amino acids to indole-3-acetic acid. Plant Cell **17:** 616–627

Stuhlfelder C, Mueller MJ, Warzecha H (2004) Cloning and expression of a tomato cDNA encoding a methyl jasmonate cleaving esterase. Eur J Biochem **271:** 2976–2983

Tan X, Calderon-Villalobos LIA, Sharon M, Zheng C, Robinson CV, Estelle M, Zheng N (2007) Mechanism of auxin perception by the TIR1 ubiquitin ligase. Nature **446:** 640–645

Teale WD, Paponov IA, Palme K (2006) Auxin in action: signalling, transport and the control of plant growth and development. Nat Rev Mol Cell Biol **7:** 847–859

Thompson JD, Gibson TJ, Plewniak F, Jeanmougin F, Higgins DG (1997) The clustalx windows interface: flexible strategies for multiple sequence alignment aided by quality analysis tools. Nucleic Acids Res **24:** 4876–4882

Ulmasov T, Murfett J, Hagen G, Guilfoyle TJ (1997) Aux/IAA proteins repress expression of reporter genes containing natural and highly active synthetic auxin response elements. Plant Cell **9:** 1963–1971

Vandenbussche F, Verbelen P, Van Der Straeten D (2005) Of light and length: regulation of hypocotyl growth in Arabidopsis. Bioessays **27:** 275–284

Varbanova M, Yamaguchi S, Yang Y, McKelvey K, Hanada A, Borochov R, Yu F, Jikumaru Y, Ross J, Cortes D, et al (2007) Methylation of gibberellins by *Arabidopsis* GAMT1 and GAMT2. Plant Cell **19:** 32–45

Walden AR, Walter C, Gardner RC (1999) Genes expressed in *Pinus radiata* male cones include homologs to anther-specific and pathogenesis response genes. Plant Physiol **121:** 1103–1116

Woodward AW, Bartel B (2005) Auxin: regulation, action, and interaction. Ann Bot (Lond) **95:** 707–735

Wu J, Wang L, Baldwin I (2008) Methyl jasmonate-elicited herbivore resistance: does MeJA function as a signal without being hydrolyzed to JA? Planta **227:** 1161–1168

Yang Y, Varbanova M, Ross J, Wang G, Cortes D, Fridman E, Shulaev V, Noel JP, Pichersky E (2006a) Methylation and demethylation of plant signaling molecules. *In* JT Romeo, ed, Recent Advances in Phytochemistry, Ed 1, Vol 40. Elsevier Science, Oxford, p 253

Yang Y, Yuan JS, Ross J, Noel JP, Pichersky E, Chen F (2006b) An *Arabidopsis thaliana* methyltransferase capable of methylating farnesoic acid. Arch Biochem Biophys **448:** 123–132

Zhao N, Ferrer J, Ross J, Guan J, Yang Y, Pichersky E, Noel JP, Chen F (2008) Structural, biochemical and phylogenetic analyses suggest that indole-3-acetic acid methyltransferase is an evolutionarily ancient member of the SABATH family. Plant Physiol **146:** 455–467

Zhao Y, Hull AK, Gupta NR, Goss KA, Alonso J, Ecker JR, Normanly J, Chory J, Celenza JL (2002) Trp-dependent auxin biosynthesis in Arabidopsis: involvement of cytochrome P450s CYP79B2 and CYP79B3. Genes Dev **16:** 3100–3112

Zhao YD, Christensen SK, Fankhauser C, Cashman JR, Cohen JD, Weigel D, Chory J (2001) A role for flavin monooxygenase-like enzymes in auxin biosynthesis. Science **291:** 306–309

Zimmerman P, Hitchcock AE (1937) Comparative effectiveness of acids, esters, and salts as growth substances and methods of evaluating them. Contrib. Boyce Thompson Inst **8:** 337–350

Zubieta C, Ross JR, Koscheski P, Yang Y, Pichersky E, Noel JP (2003) Structural basis for substrate recognition in the salicylic acid carboxyl methyltransferase family. Plant Cell **15:** 1704–1716